RESEARCH ARTICLE

A Simple Flow-Cytometric Method Measuring B Cell Surface Immunoglobulin Avidity Enables Characterization of Affinity Maturation to Influenza A Virus

Gregory M. Frank,[a] Davide Angeletti,[a] William L. Ince,[a] James S. Gibbs,[a] Surender Khurana,[b] Adam K. Wheatley,[c] Edward E. Max,[d] Adrian B. McDermott,[c] Hana Golding,[b] James Stevens,[e] Jack R. Bennink,[a] Jonathan W. Yewdell[a]

Laboratory of Viral Diseases, National Institute of Allergy and Infectious Diseases, National Institutes of Health, Bethesda, Maryland, USA[a]; Center for Biologics Evaluation and Research, Food and Drug Administration, Silver Spring, Maryland, USA[b]; Vaccine Research Center, National Institute of Allergy and Infectious Diseases, National Institutes of Health, Bethesda, Maryland, USA[c]; Center of Drug Evaluation and Research, Food and Drug Administration, Silver Spring, Maryland, USA[d]; Influenza Division, National Center for Immunization and Respiratory Diseases, Centers for Disease Control and Prevention, Atlanta, Georgia, USA[e]

ABSTRACT **Antibody (Ab) affinity maturation enables an individual to maintain immunity to an increasing number of pathogens within the limits of a total Ig production threshold. A better understanding of this process is critical for designing vaccines that generate optimal Ab responses to pathogens. Our study describes a simple flow-cytometric method that enumerates virus-specific germinal center (GC) B cells as well as their AC_{50}, a measure of Ab avidity, defined as the antigen concentration required to detect 50% of specific B cells. Using a model of mouse Ab responses to the influenza A virus hemagglutinin (IAV HA), we obtained data indicating that AC_{50} decreases with time postinfection in an affinity maturation-dependent process. As proof of principle of the utility of the method, our data clearly show that relative to intranasal IAV infection, intramuscular immunization against inactivated IAV in adjuvant results in a diminished GC HA B cell response, with increased AC_{50} correlating with an increased serum Ab off-rate. Enabling simultaneous interrogation of both GC HA B cell quantity and quality, this technique should facilitate study of affinity maturation and rational vaccine design.**

IMPORTANCE **Though it was first described 50 years ago, little is known about how antibody affinity maturation contributes to immunity. This question is particularly relevant to developing more effective vaccines for influenza A virus (IAV) and other viruses that are difficult vaccine targets. Limitations in methods for characterizing antigen-specific B cells have impeded progress in characterizing the quality of immune responses to vaccine and natural immunogens. In this work, we describe a simple flow cytometry-based approach that measures both the number and affinity of IAV-binding germinal center B cells specific for the IAV HA, the major target of IAV-neutralizing antibodies. Using this method, we showed that the route and form of immunization significantly impacts the quality and quantity of B cell antibody responses. This method provides a relatively simple yet powerful tool for better understanding the contribution of affinity maturation to viral immunity.**

Received 10 July 2015 **Accepted** 14 July 2015 **Published** 4 August 2015

Citation Frank GM, Angeletti D, Ince WL, Gibbs JS, Khurana S, Wheatley AK, Max EE, McDermott AB, Golding H, Stevens J, Bennink JR, Yewdell JW. 2015. A simple flow-cytometric method measuring B cell surface immunoglobulin avidity enables characterization of affinity maturation to influenza A virus. mBio 6(4):e01156-15. doi:10.1128/mBio.01156-15.

Editor Gary J. Nabel, Sanofi

Address correspondence to Jonathan W. Yewdell, jyewdell@mail.nih.gov.

G.M.F. and D.A. contributed equally to this work.

This article is a direct contribution from a Fellow of the American Academy of Microbiology.

Antibodies (Abs) are a critical component of the immune response to viruses. Abs accelerate viral clearance in primary infections and often provide life-long immunity to subsequent infections with antigenically similar viruses. As with every biological function, the capacity of the immune system to synthesize Abs is finite. Total serum Ig concentrations in mammals are typically maintained near 12 mg/ml, with only minor increases associated with aging (1). Since serum Abs may be induced by thousands of pathogens during a long life span, the efficacy of Abs specific for each pathogen is at a premium. Efficiency is optimized by the process of Ab affinity maturation (2). A thousandfold increase in Ab affinity implies (this has never been carefully tested) that 1,000-fold less antibody would exert an equal biological effect.

During Ab affinity maturation, activated naive B cells form structures called germinal centers (GC), where, with appropriate T cell help, they randomly diversify their Ab-encoding genes. Higher-affinity clones win the competition for survival and spawn long-lived plasma cells and memory B cells, which when activated can experience further affinity maturation (3, 4).

Historically, characterization of B cell responses has been largely limited to measuring Ab responses in serum and secretions and sequencing antigen-specific Ig genes from B cell hybridomas. Recent advances enable discrimination of B cells according to an-

tigen binding and activation status (5–7). New techniques rapidly characterize individual Ab genes from single B cells to interrogate B cell populations (8–10). These advances are creating a revolution in the understanding of B cell immunity.

Here, we studied B cell responses to influenza A virus (IAV), a leading cause of death in the United States, with associated yearly costs of roughly $50 billion. It is particularly important to understand Ab responses to IAV. Rapid evolution of the hemagglutinin (HA), the target of the most potent virus-neutralizing Abs (11, 12), necessitates frequent updates to vaccine formulation and limits vaccine efficacy, particularly in the elderly (13, 14).

Pioneering DNA sequencing of Ab genes from HA-specific hybridomas by Gerhard, Caton, Weigert and colleagues provided the initial information on the diversity of Ab gene usage in B cell responses to pathogens (15). Later research built on this foundation by establishing the validity of using fluorescent HA to identify specific B cells by flow cytometry (16) and using HA-based B cell sorting to determine HA-specific Ab sequences from single cells and populations (16–19).

Building on these advances, we developed a flow cytometry-based method that enables the characterization of surface Ig expressing GC-resident B cells following primary IAV infection and immunization. We demonstrate and validate that by titrating a recombinant IAV protein hemagglutinin (HA) probe while staining B cells, we can also derive a measure of the population's antibody avidity for HA, defined as the antigen concentration required to detect 50% of HA-specific B cells (AC_{50}). We can show that AC_{50} decreases over time and its change is due to affinity maturation. As proof of principle of the power of this simple yet robust approach, we demonstrate that pulmonary infection induces a quantitatively and qualitatively superior Ab response compared to the standard route of vaccination by intramuscular (i.m.) injection. This approach enables simultaneous measurement of the GC B cell response magnitude and avidity over time and represents a powerful tool for better understanding of affinity maturation and vaccine design.

RESULTS

Recombinant HA can specifically identify HA-specific GC B-cells. To identify HA-specific B cells, we used recombinant HA from A/Puerto Rico/8/34 (PR8) secreted by insect cells with its carboxy-terminal domain modified to promote trimerization and enable detection with an anti-His tag monoclonal antibody (MAb). This HA preparation (rHA^{PR8}) is remarkably native, as shown by biochemical analysis in conjunction with a panel of MAbs to assess conformation (20). To establish the properties of rHA^{PR8} as a B cell probe, we screened hybridoma cell lines to identify a line that expresses cell surface Ig, which is unusual (21). H17-L7, an HA Cb site-specific hybridoma, exhibits surface IgG expression (Fig. 1A) and binds rHA^{PR8} in a dose-dependent fashion but does not bind to the serologically distant H5 $rHA^{Vietnam\ 04}$, demonstrating the specificity of staining with rHA^{PR8} (Fig. 1B and C).

We next stained mediastinal lymph node (MLN)-resident B cells from B6 mice infected intranasally (i.n.) with PR8. We focused on GC B cells (defined as $B220^+$ $CD38^{lo}$ $GL7^{hi}$), as they exhibit a distinct differentiation marker profile and retain strong surface Ig expression (22). Among MLN CD3-negative cells (>90% $B220^+$), rHA^{PR8} staining was essentially limited to GC B cells (Fig. 1D). To confirm the specificity of rHA^{PR8} binding to GC B cells, we infected mice with a reassortant IAV (J1) with 7 PR8 genes but a serologically distinct HA from an H3 virus (A/Hong Kong/1/68). Little reactivity was observed from J1-infected GC B cells up to an rHA^{PR8} concentration of 66 nM, providing an upper concentration limit for detecting Ab-specific binding of this probe to GC B cells (Fig. 1E).

HA-specific GC B cells exhibit different responses in local versus central lymphoid organs. Using a staining concentration of 66 nM rHA^{PR8} we quantified the HA-specific GC B cell response following i.n. infection in the MLNs and spleen. HA-specific GC B cells were first detected at 7 days postinfection (dpi) in MLNs and 10 dpi in the spleen. Numbers of splenic HA-reactive GC B cells peaked at 14 dpi, while their MLN-resident counterparts peaked a week later (Fig. 2A). Expressed as a fraction of total GC B cells, splenic B cells peaked at 21 dpi while MLN B cells continued to rise in frequency at 28 dpi (Fig. 2B).

These findings confirm the utility of rHA^{PR8} in tracking HA-specific responses and clearly demonstrate distinct kinetics of the HA-specific GC B cell response in proximal versus distal lymphoid organs.

AC_{50} of HA-specific GC B cells can be used as a proxy for population avidity for PR8 HA. As initially described for hapten-specific B cells (23), the binding of rHA^{PR8} to GC B cells should obey the law of mass action and thereby provide a measure of Ab affinity for HA. In theory, for any B cell, Ab affinity should equal the rHA^{PR8} concentration that gives half-maximal binding ($rHA^{PR8}{}_{50}$). There is no need to reach saturation to define AC_{50}, as B cell receptor (BCR)-specific and "nonspecific" antigen binding is a continuum, where "nonspecific" means low-affinity binding of germline BCRs. However, during an immune response, Abs with high affinity will outcompete those with lower affinity. Therefore, our maximum binding is the binding at a concentration where naive BCRs do not bind. While each B cell can be tested only for binding to a single rHA^{PR8} concentration, at the population level, if cell surface Ig levels are equally distributed among B cell clones, the average Ab affinity will track the rHA^{PR8} concentration that detects half the number of HA-specific B cells. We define this as the 50% antigen concentration (AC_{50}) (Fig. 3A). It is important to emphasize that since HA-specific GC B cells comprise a heterogeneous population of clones with various affinities and surface Ig expression, AC_{50} provides (at best) the mean affinity of Abs expressed by the HA-specific B cell population studied.

We verified the validity of AC_{50} measurements by comparing the calculated H17-L7 AC_{50} versus purified H17-L7 MAb affinity determined via ELISA (Fig. 3B). We observed remarkable agreement between AC_{50} (1.1 nM) and K_D (equilibrium dissociation constant) (0.6 nM), supporting the validity of our approach. We next compared the avidities of 10 MAbs generated 5 days after primary infection (24) to the AC_{50} of GC B cells 7 days after i.n. infection. Again, there was strong concordance of AC_{50} with the average avidity, with both values being ~10 nM (Fig. 3D).

We next investigated the extent to which the AC_{50} is influenced by the fraction of HA-specific cells in a B cell population, an important factor given the low and variable fraction of HA-specific B cell in *ex vivo* populations used for studying HA-specific GC B cell responses. We mixed naive splenocytes with H17-L7 hybridoma in different proportions and determined the binding curves and respective AC_{50}s. The AC_{50}s were statistically indistinguishable between the different mixtures (Fig. 3E).

Based on these findings, we conclude that by simple antigen

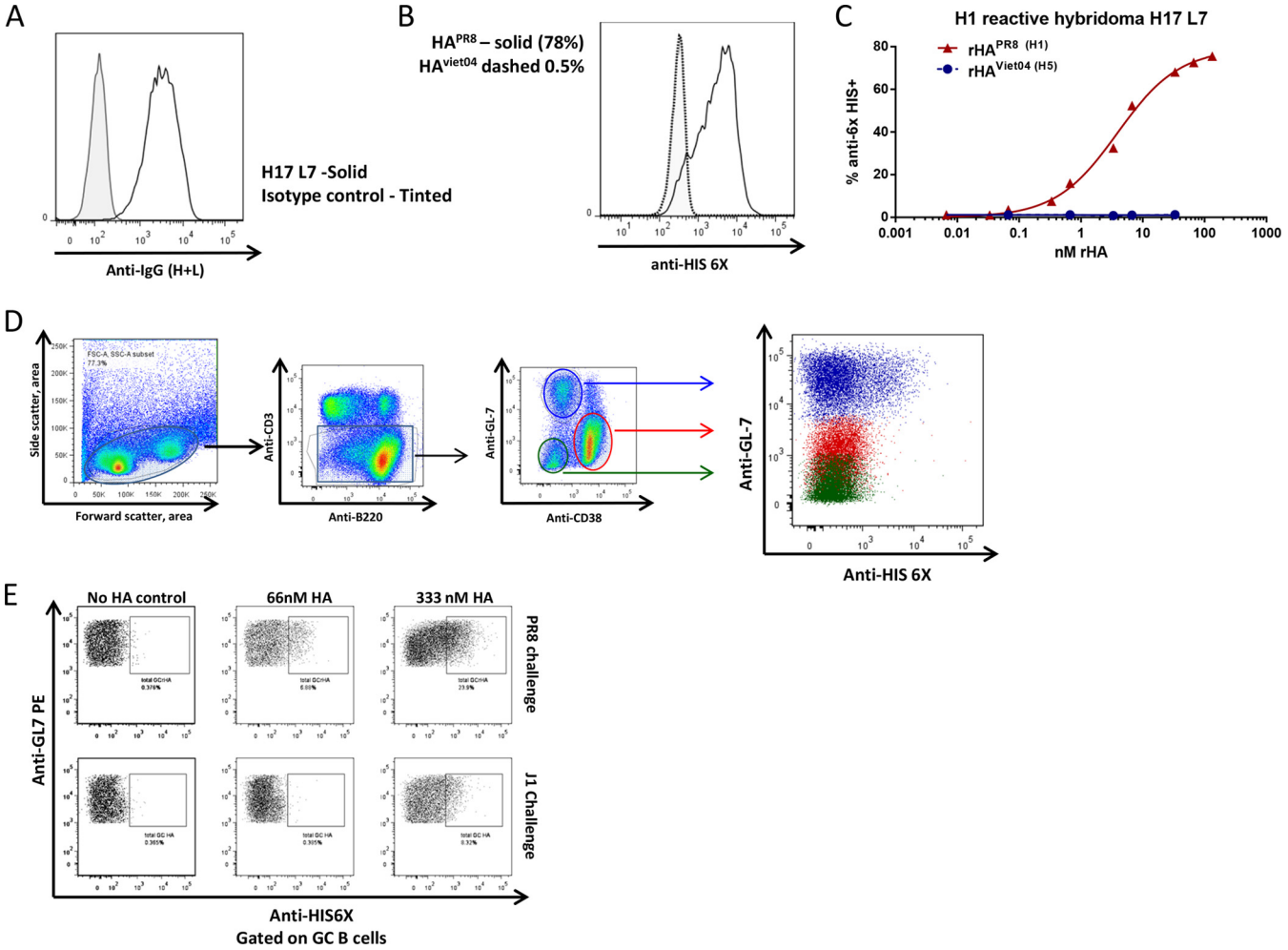

FIG 1 Recombinant HA can specifically identify HA-specific GC B cells. Briefly, we treated cells with receptor-destroying enzyme for 60 min at 37°C to remove sialic acid from the cell surface to minimize nonspecific binding. We stained cells first with surface MAb, then with rHA, and finally with anti-6×His MAb to detect rHA binding. (A) Representative flow plots demonstrate that H17 L7, a PR8 HA-specific hybridoma, retains high levels of surface Ig expression. (B) Representative flow plots indicate that H17 L7 binds strongly to A/Puerto Rico/8/1934 molecular clone rHA (rHA^{PR8}) but not to A/Vietnam/1203/2004 rHA ($rHA_{Viet\ 04}$), a serologically distinct HA. (C) Plot of percent 6×His-positive cells versus rHA^{PR8} concentration illustrating that H17 L7 reacts to rHA^{PR8} in a dose-dependent fashion. At 14 days after PR8 i.n. infection, MLNs were excised and dispersed into single-cell suspensions, and GC B cells were stained using the rHA approach. (D) representative plots depict gating strategy to observe GC B cells based on $B220^{+}$ $GL\text{-}7^{+}$ $CD38^{-}$ surface expression. Only GC B cells reacted specifically to rHA^{PR8}. (E) B6 mice were i.n. infected with an H3N1 reassortant (J1), and MLN-resident GC B cells were stained with rHA^{PR8}. Representative flow plots of MLN resident GC B cell 6×His staining show that J1-responding GC B cells did not react to rHA^{PR8} at staining concentrations up to 66 nM, providing the maximum staining concentration of rHA^{PR8} that can be used to identify H1 HA-specific B cells with confidence. Data represent 3 independent experiments.

titration in flow-cytometric staining, we can derive a value, the AC_{50}, that provides a measure of the affinity of the B cell Ig receptor.

AC_{50} characterization of HA-specific GC B cells. We next used AC_{50} to characterize maturation of specific GC B cell responses in MLNs and spleens during IAV infection. GC B cells at 28 dpi had a significantly higher frequency of HA reactivity at lower rHA^{PR8} concentrations than 14-dpi counterparts (Fig. 4A), with a clear increase in HA-specific GC B cell frequency and a decrease of AC_{50} over 4 weeks following infection (Fig. 4B). AC_{50} decreased approximately 30-fold, from 10 nM at 7 dpi to 0.36 nM at 28 dpi (Fig. 4C).

While we were unable to obtain reliable AC_{50} data for spleen-resident B cells at early and late time points due to low frequencies of HA-specific GC B cells (Fig. 2B), we did calculate AC_{50} at 14 and 21 dpi, which follow a surprisingly similar pattern of AC_{50} decrease to MLN-resident GC B cells (Fig. 4D). Importantly, we cannot trivially attribute the time-dependent decrease of AC_{50} in MLN and splenic GC B cells to temporal increases in GC B cell surface Ig levels, which are statistically indistinguishable between 14 and 28 dpi (Fig. 4E) (note that likely due to steric hindrance, we were unable to costain GC B cells with rHA^{PR8} and anti-Ig Abs to directly correlate Ig surface levels with antigen binding).

A potential pitfall of HA staining is the requirement to treat cells with neuraminidase to prevent HA binding to the abundant cell surface terminal sialic acids. To circumvent this problem, we used an rHA with a substitution in the sialic acid binding site that prevents sialic acid binding ($rHA^{PR8\text{-}Y98F}$) (19). This enabled GC B cell staining without neuraminidase treatment of cells and gave

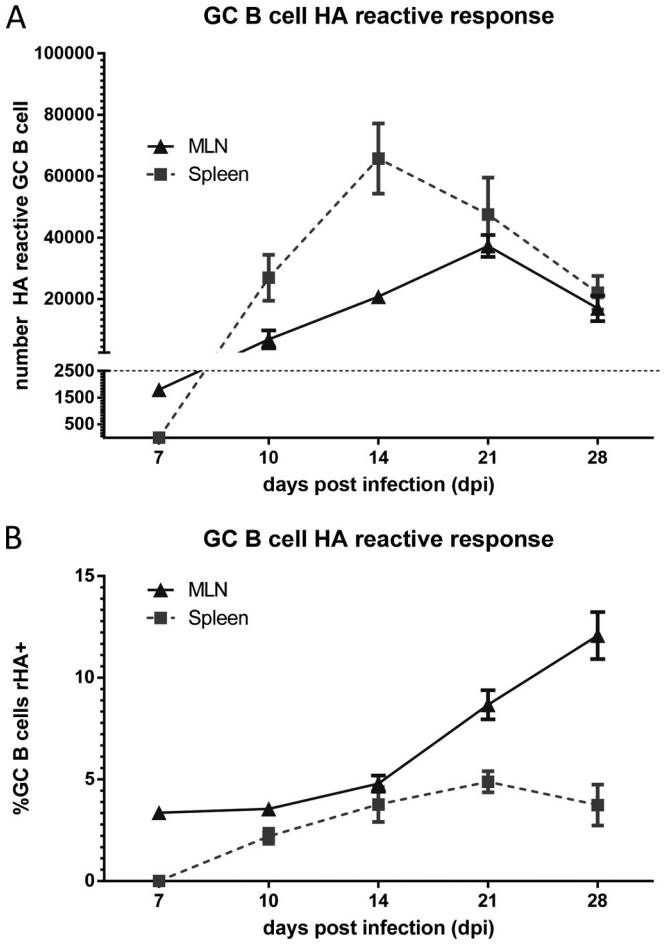

FIG 2 HA-specific GC B cells exhibit different responses in local versus central lymphoid organs. At the indicated times after PR8 i.n. infection, we removed MLN or spleens, dispersed them into single-cell suspensions, and stained GC B cells with rHA. Line graphs indicate the absolute number (A) and frequency (B) of GC B cells specifically binding rHA^{PR8} (based on a staining concentration of 66 nM) over time in the MLNs and spleens. MLN GC B cells binding rHA^{PR8} form earlier (7 dpi) but peak later (21 dpi) than spleen-resident GC B cells, which do not appear until after 7 dpi and peak at 14 dpi. Data are representative of 3 to 6 independent experiments.

essentially identical results (see Fig. S1 in the supplemental material).

Using the $rHA^{PR8\text{-}Y98F}$ probe, it was further possible to costain with anti-Ig Abs, allowing us to correlate IgG surface levels and rHA binding. We show that the amount of IgG on the surface of B cells does not determine rHA binding (see Fig. S2 in the supplemental material), strengthening our conclusion that AC_{50} is not trivially due to different levels of surface B cell receptor.

Lastly, we used the mean fluorescent intensity (MFI) of stained cells to calculate the AC_{50}. As predicted from the law of mass action, this yielded results similar to those obtained by using the percent positive cells (an example is shown in Fig. S3 in the supplemental material) but exhibited greater variability between samples. Therefore, in all additional experiments, we calculated the AC_{50} based on the percent positive cells.

AC_{50} increase is driven by affinity maturation. If the observed decrease in AC_{50} is due to affinity maturation, it should not occur in mice with activation-induced deaminase knockout ($AID^{-/-}$ mice), which are incapable of somatic hypermutation (25). In response to intrperitoneal (i.p.) injection of UV light-inactivated PR8, WT mice generated a robust HA-specific GC B cell response exhibiting 12-fold-decreased AC_{50} (5.8 nM to 0.49 nM) between 14 and 28 dpi (Fig. 5A and B). As seen in other studies, the $AID^{-/-}$ mice generate a large germinal-center reaction, with a robust HA-specific GC B cell response (26). However, the $AID^{-/-}$ response's AC_{50} remained constant from 14 to 28 dpi (Fig. 5). Since Ig class switching is also abrogated in $AID^{-/-}$ mice, these data strongly support the conclusion that kinetic changes in AC_{50} reflect the selection of higher-affinity HA-specific clones by classical B cell somatic mutation and selection mechanisms.

Intramuscular vaccination with inactivated PR8 and adjuvant produces an inferior HA-specific GC B cell response. As proof of principle of the utility of AC_{50} for characterizing immune responses, we compared i.n. infection with infectious PR8 to a single intramuscular (i.m.) injection of UV-inactivated PR8 in Titermax adjuvant. The latter is known to be less protective against lethal PR8 challenge (27). Following i.m. immunization, serum anti-HA Abs were always detected, confirming successful vaccination (data not shown). HA-specific GC B cell responses were uniformly observed in the most proximal popliteal draining lymph nodes, 33% of the time in the more distant inguinal nodes, but never within the spleen (Fig. 6A), indicating only localized generation of HA-reactive GC B cells.

The HA-specific B cell response in the inguinal LN was similar in frequency to that in i.n. infection (Fig. 6B) but was numerically inferior; i.m. vaccination of mice induced only 5% and 7% of GC B cells compared to i.n. infection at 14 and 28 dpi, respectively (Fig. 6C). While the popliteal LN B cell numbers induced by i.m. immunization were too low to establish AC_{50} due to lymph node size, the inguinal LN GC B cell response decreases in AC_{50} from 14 to 28 after i.m. vaccination with similar kinetics to infected responses (~7 to 10-fold decrease, vaccination to infection, respectively). However, at both time points, the GC B cell AC_{50} after vaccination was approximately 4-fold higher than those responding to i.n. infection (Fig. 6D). Thus, i.m. vaccination resulted in a 14- to 20-fold lower HA-specific GC B cell response that was also 4-fold higher in AC_{50} than that achieved with i.n. infection.

These findings predict that i.m. immunization will generate less anti-HA Ab of lower affinity. We tested this prediction by surface plasmon resonance (SPR) analysis of serum Ab responses, which provides a measure of total Ab responses and accurately measures the average Ab off-rates, typically the most important factor in Ab affinity. In agreement with our measurement of GC B cell numbers, serum antibody HA-binding activity from i.m.-vaccinated mice was 38% and 17% lower than in sera from infected animals at 14 dpi and 28 dpi, respectively (Fig. 6E). Further confirming our AC_{50} data, Ab off-rates decreased in vaccinated mice between days 14 and 28, suggesting increased affinity, but retained statistically significant faster off-rates compared to postinfection sera (Fig. 6F). The disparity in off-rates (1.3-fold and 1.4-fold higher at days 14 and 28 postvaccination, respectively) remained stable relative to values for postinfection sera, similar to observed GC B cell AC_{50} (Fig. 6D).

Taken together, these data support the validity of the AC_{50} method for determining Ab avidity and demonstrate its utility for analyzing immunity to viral infection and immunization.

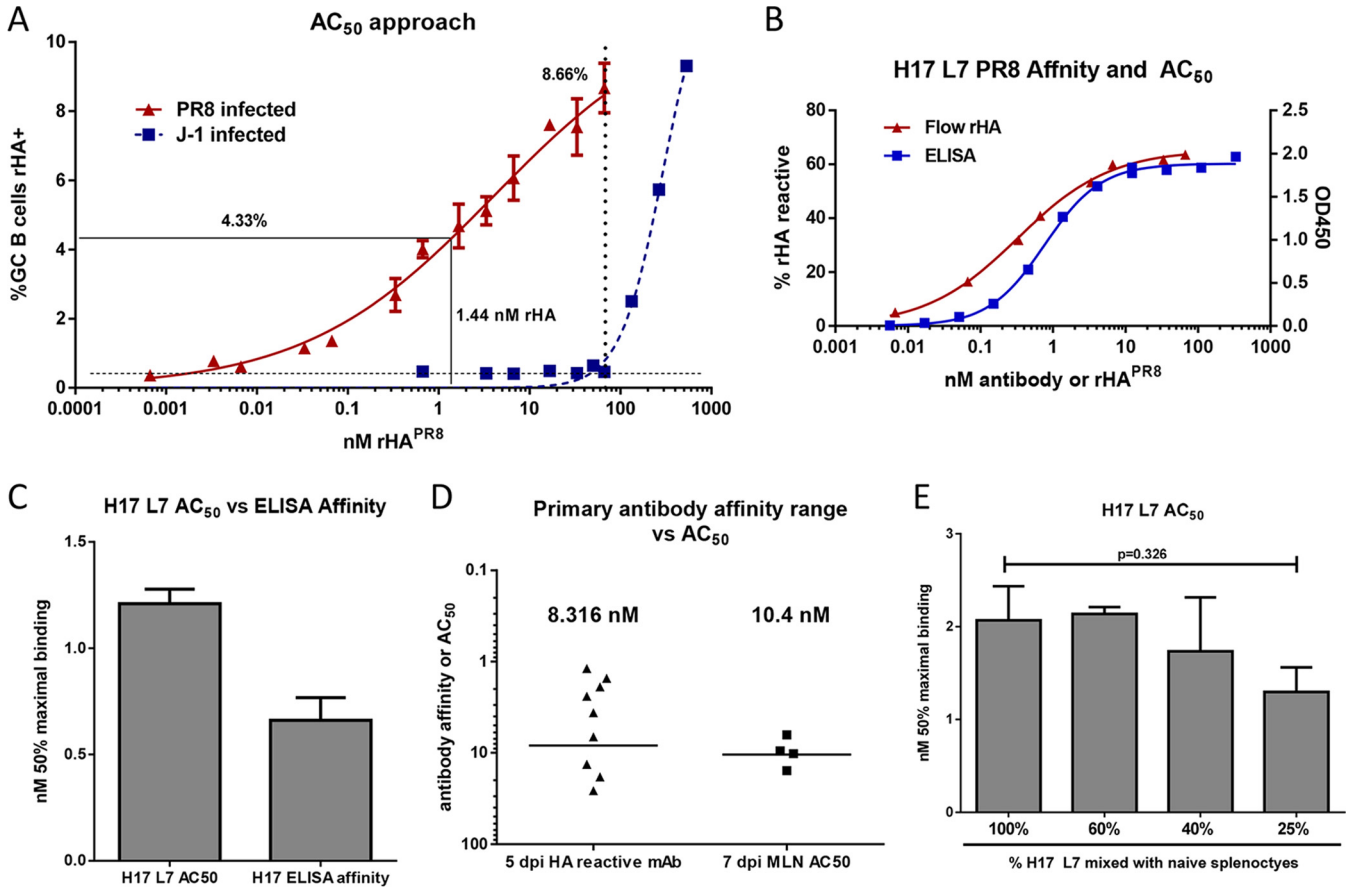

FIG 3 AC_{50} of HA-specific GC B cells can be used as a proxy for population avidity to PR8 HA. (A) Overview of AC_{50}. GC B cell rHA staining frequency is plotted against rHA^{PR8} concentration. Nonspecific binding by J1-responding GC B cells occurs at concentrations above 66 nM rHA^{PR8}. Using this dose as the maximum specific staining of HA-specific GC B cells, we estimated the half-maximal specific binding rHA^{PR8} concentration. This provides a molar rHA^{PR8} value we call the AC_{50}, a proxy measurement of population avidity for rHA^{PR8}. (B) Representative titration curve of H17 L7 HA-specific hybridoma using rHA^{PR8} (red plots) or by ELISA of purified H17 L7 antibody to plated whole virus (blue plots). (C) Bar graph depicting the calculated AC_{50} compared to ELISA affinity. Values are within 1.8-fold of each other. (D) Comparison of HA-specific GC B cell AC_{50}, 7 days after PR8 i.n. infection, with mean affinity of 9 different 5-dpi MAbs. The AC_{50} and mean affinity are statistically indistinguishable. (E) AC_{50} for H17 L7 HA-specific hybridoma mixed in different proportions with naive splenocytes and assayed using rHA^{PR8}. AC_{50} is independent of the proportion of specific cells. Data are representative of 2 or 3 independent experiments.

DISCUSSION

While a large body of research carried out over decades supports the importance of HA-specific antibody in the control of IAV infection (28), little is known about the immunological mechanisms that drive HA-specific B cell responses. In this study, we demonstrate how flow-cytometric characterization of HA-specific GC B cell responses provides a wealth of information on the kinetics, magnitude, and most importantly the quality of the HA B cell immune response to IAV infection.

Our approach hinges on the quality and specificity of the antigen probe used to identify B cells. We were fortunate to have collaborative access to recombinant HA preparations that are homogeneously extremely well folded (19, 20), minimizing the nonspecific binding of denatured probe to GC B cells. As Bardelli et al. originally reported (18), we found it necessary to treat GC B cells with neuraminidase to reduce nonspecific binding of rHA to tolerable levels. Neuraminidase treatment did not have a significant effect on the staining of the cell surface antigens analyzed in this study (data not shown). Using a novel rHA^{PR8} probe with a single amino acid mutation (Y98F) in the sialic acid binding site that abolishes sialic acid binding (19), we could confirm that neuraminidase treatment does not affect the accuracy of the method (see Fig. S1 in the supplemental material). Still, it is advantageous to avoid neuraminidase treatment in terms of time, expense, and reproducibility, and such receptorless HA probes are clearly preferred for all future studies (with the one caveat that they may display less binding to broadly neutralizing Abs with CDRs [complementarity determining regions] that extend into the sialic acid binding site [29]). Obviously, for other antigenic proteins, our approach is limited by the need to have a pure, well-folded, and homogeneous probe and also the requirement to prevent its binding to B cell non-Ig receptors, either by modifying the receptor properties of the probe or by removing/blocking the receptor on the B cell surface.

Our upper limit of rHA^{PR8}-specific binding was 66 nM, raising the question of how many biologically relevant lower-affinity HA-specific B cells we are missing. Since Ab binding to antigen is a continuum, there is no absolute limit between specific and nonspecific binding. Practically, however, if naive B cells generate Abs at reasonably high affinity prior to affinity maturation, this will set

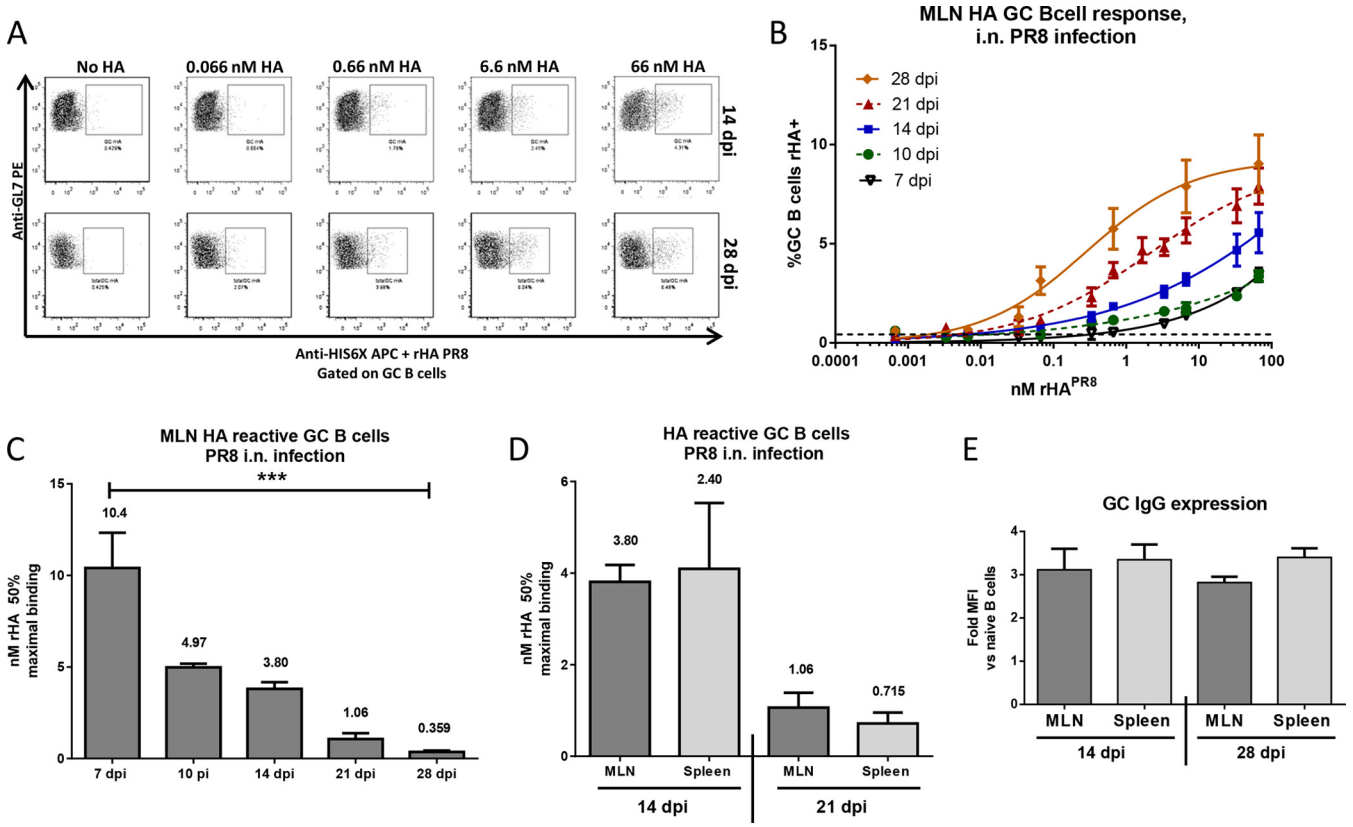

FIG 4 AC_{50} characterization of HA-specific GC B cells. At indicated times after PR8 i.n. infection, we excised MLN or spleens, dispersed them into single-cell suspensions, and stained GC B cells with rHA. (A) Representative flow plots depict MLN resident GC B cell reactivity to graded concentrations of rHA^{PR8}. GC B cells at 28 dpi react more strongly to lower staining concentrations than those at 14 dpi. (B) Titration curves of MLN-resident GC B cells to rHA^{PR8} following i.n. PR8 infection. Data represent the frequency of positive cells plotted against rHA^{PR8} concentration. (C) AC_{50} was calculated for each titration curve and is presented as the concentration (nanomolar) of rHA^{PR8} required to reach 50% maximal binding at the indicated time points. MLN-resident GC B cells decrease AC_{50} to rHA^{PR8} 29-fold between 7 and 28 days postinfection, or a 140% increase each day. (D) AC_{50} of spleen-resident GC B cells at 14 and 21 dpi following i.n. infection. Despite different frequencies and kinetics of response, HA AC_{50} is similar to that of MLN GC B cells. (E) At 14 and 28 dpi, MLNs were excised, dispersed into single-cell suspensions, and stained with anti-IgG Fcγ MAb. The graph illustrates normalized MFI levels of IgG Fcγ expression of GC B cells relative to naive B cells that express no IgG (set as baseline MFI) at 14 and 28 dpi. No significant difference in per-cell-surface IgG expression occurs between 14 and 28 days postinfection. All data are representative of 3 to 7 replicate experiments.

a biologically relevant affinity threshold for relevant affinities, since they will outcompete Abs with lower affinities during the immune response. For PR8 HA, we found that B6 mice possess enough naive B cells expressing Abs with K_D of 1×10^{-8} M to generate a strong response by simply expanding these cells by 5 to 7 dpi (Fig. 3D). This is consistent with studies that examined 6-dpi primary affinities of mouse MAbs specific for HA (24) or the equivalent receptor protein from vesicular stomatitis virus (24, 30). Further, naive humans seem to generate Abs to IAV HA with a similar affinity range (10). To place this affinity into functional context, half of HA epitopes will be bound when serum reaches an Ab concentration of 10 nM (10^{-8} M, or 6×10^{12} molecules/ml). Fifty years ago, Fazekas de St. Groth reported that by day 14 following immunization, rabbits already possessed up to 10^{15} Abs/ml (31). Thus, even without affinity maturation, primary Ab responses to HA should exert considerable biological activity. Therefore, while it is certain that we are missing a substantial number of low-avidity B cells, it is likely that the Ab with K_D at or below 10 nM that we detect are the most biologically relevant species responding to IAV.

Given that the overall Ab response to IAV appears to be highly biased toward HA (15), it is surprising that HA-specific cells seem to comprise a small fraction of GC B cells (15% or less). There are several possible explanations, each of which likely contributes to this observation. First, although GCs are induced by virus, this does not guarantee that every activated B cell in the GC was activated by IAV antigens. It is possible that IAV infection induces a self-specific response, and we cautiously remind readers that a Nobel Prize was awarded to Jerne for his theory that Ab responses induce a strong anti-idiotypic response (32, 33), though there could be many other self antigens of greater importance.

Second, we are unaware of definitive data on the relative abundance of antibodies specific for various IAV gene products (or other viruses). Though M1 and the polymerases are not highly immunogenic, NP and NS1 are clearly major immunogens following live virus infection (34). Further, many hybridomas isolated from IAV-immunized mice by Gerhard and colleagues were specific for poorly defined glycolipid components of the host cells used to grow the virus (35).

Third, our rHA^{PR8} preparation clearly is not identical to HA in the immunizing virus. The rHA^{PR8} is folded with remarkable fidelity, but as an insect cell product, it lacks the complex carbohy-

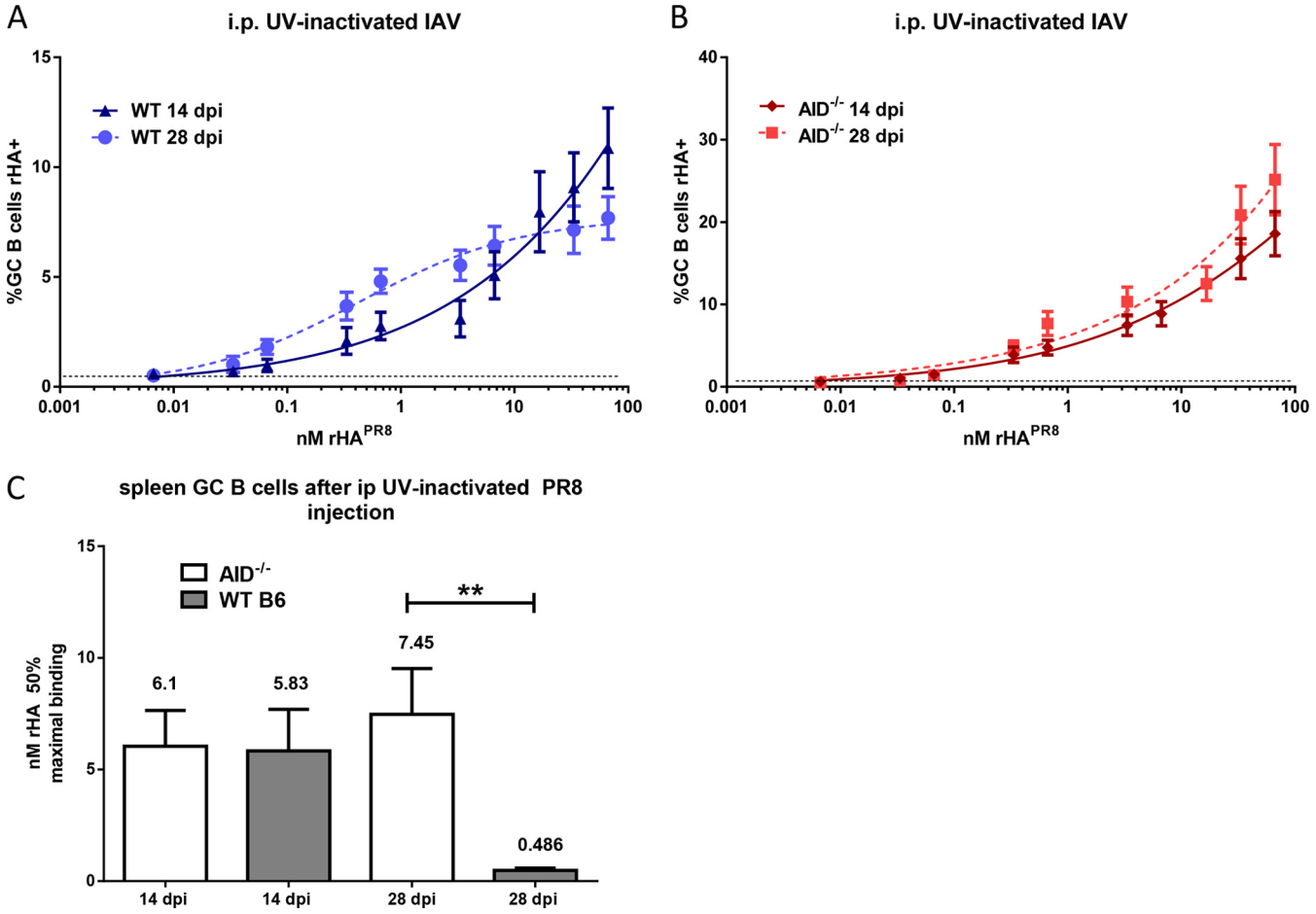

FIG 5 AC_{50} decrease is driven by affinity maturation. We injected B6 and $AID^{-/-}$ mice i.p. with UV-inactivated PR8, and 14 and 28 days later, we excised spleens and dispersed them into single-cell suspensions. We then stained GC B cells with rHA. (A and B) Titration of B6 GC B cells and $AID^{-/-}$ GC B cells, respectively, using rHA^{PR8} at 14 and 28 dpi, plotting the frequency of positive cells versus rHA^{PR8} concentration. (C) AC_{50} was calculated for each titration curve and is presented as the concentration (nanomolar) of rHA^{PR8} required to reach 50% maximal binding at indicated time points. While WT GC B cells decrease AC_{50} to rHA^{PR8} by 12-fold between 14 and 28 days postinfection, $AID^{-/-}$ GC B cell AC_{50} remains stable. Data are representative of 3 independent experiments.

drates present on HA produced by vertebrate cells (36). However, it should be noted that $rHA^{PR8\text{-}Y98F}$, expressed from a mammalian cell line, should have complex carbohydrates and detects a similar frequency of reactive B cells. As soluble proteins, both probes would be unable to detect MAbs that require the geometric array of HA present on virions or infected cell material.

Fourth, GC B cell makeup may not accurately predict GC-derived plasma cell frequency, and our current staining approach does not interrogate the GC-independent extrafollicular plasma cell response, which has been observed in B6 mice following IAV infection (37). Further study will be required to better correlate the HA-reactive GC B cell response to HA-reactive serum Abs.

We observed distinct kinetics of HA-specific GC B cells when comparing the MLN and the spleen. While HA-specific GC B cells were detected earlier in the MLN (7 dpi), the splenic HA-specific GC response peaked earlier and was larger in magnitude (Fig. 2A) but contained a smaller fraction of HA-specific cells (Fig. 2B). Boyden et al. (38) reported prominent differences in local versus central GC responses to pulmonary IAV infection. Differential kinetics of antigen delivery (39) likely contributes to this phenomenon, but there are probably also local factors, including the nature and magnitude of help provided by follicular T helper cells.

The MLN GC HA-specific response AC_{50} increases approximately 30-fold between 7 and 28 dpi (Fig. 4C), a process that is almost certainly driven by affinity maturation, as indicated by the stable AC_{50} in $AID^{-/-}$ mice over time (Fig. 5C). Outside the pioneering efforts of Fazekas de St. Groth (31), there are surprisingly limited data on the degree of affinity maturation of antiviral responses or its biological effects. It is notoriously difficult to determine the average affinity of Ab responses in biological fluids, where the amount of the specific Ab is difficult to determine. Indeed, this was one of the driving factors for our developing the AC_{50} approach. Admirably eager to challenge dogma, Roost and colleagues reported the absence of Ab affinity maturation in mouse responses to vesicular stomatitis virus (VSV) (30), and Zinkernagel questioned its relevance to antiviral immune responses (40).

Our AC_{50} of 1 nM for 21-dpi responses in mice is in good agreement with values from Fazekas de St. Groth et al. (41), who observed average Ab dissociation constants of 0.75 nM for 21-dpi responses to PR8 in rabbits (note that this is after conversion from the CGS units typically used by Fazekas de St. Groth in his publications). Recent studies using SPR analysis demonstrate that Ab off-rates decline in humans following IAV immunization (42),

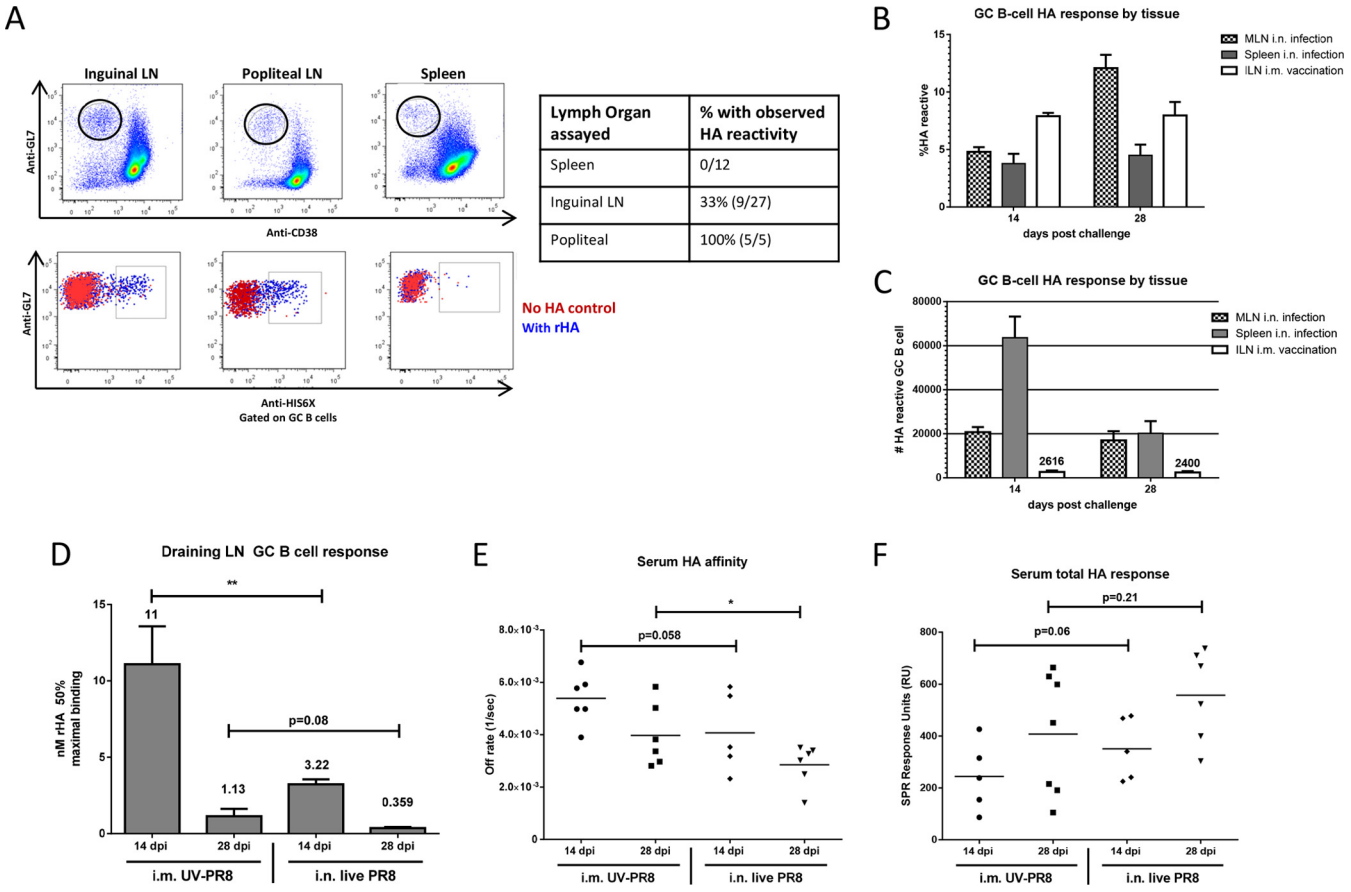

Lymph Organ assayed	% with observed HA reactivity
Spleen	0/12
Inguinal LN	33% (9/27)
Popliteal	100% (5/5)

FIG 6 Intramuscular vaccination with inactivated PR8 and adjuvant produces an inferior HA-specific GC B cell response. We injected mice bilaterally with a total dose of 2.5×10^7 $TCID_{50}$/mouse (pre-UV inactivation) diluted 1:1 with Titermax gold adjuvant or infected mice i.n. with 50 $TCID_{50}$ per mouse. At 14 and 28 dpi, we removed lymphoid organs draining the site of injection, the inguinal LN, and/or popliteal LN (i.m. vaccination) or mediastinal LN (i.n. infection), and spleens, dispersed them into single-cell suspensions, and stained GC B cells with rHA. (A) Representative flow plots depict total GC B cell response (top) as well as HA binding (bottom). Red dot plots indicate no HA control staining, while blue dot plots represent HA staining at 66 nM rHA^{PR8}. The table depicts the frequency with which an HA-specific GC B cell response was seen in the lymphoid organ following i.m. vaccination. (B and C) Bar graphs depicting numbers of HA-specific GC B cells and frequency of HA-specific GC B cells per tissue. Mice vaccinated i.m. have sporadic distal LN involvement and no splenic HA response, while productively infected mice have large HA-specific populations in the draining MLN as well as the distal spleen. (D) AC_{50} for each condition. GC B cells responding to i.m. vaccination have ~4-fold-higher AC_{50} than those formed to productive i.n. infection. Scatter plots of HA binding signal (E) and Ab off-rate (F). Serum from 14 and 28 days after i.m. PR8-vaccinated and i.n. PR8-infected mice were tested by surface plasmon resonance (SPR) analysis to determine Ab signal and off-rates. Serum from i.m.-vaccinated mice had an amount of HA binding antibody and had significantly higher off-rates at both 14 and 28 dpi. Data are representative of 2 to 4 independent experiments.

extending previous work using resistance to denaturants to roughly measure Ab avidity (43). An enormous volume of new data from MAbs obtained from human B cells conclusively links increased affinity with somatic hypermutation (44–46). Thus, the doubts about the relevance of Ab affinity maturation in antiviral immunity expressed by Zinkernagel (40) are not supported by more recent studies.

AC_{50} determination enables rapid comparisons of the kinetics and affinity quality of HA responses to a variety of source antigens, e.g., inactivated viral immunogens used for vaccination. There is considerable room for improvement in IAV vaccination, which at best provides only partial protection even in years with good antigenic matching of vaccine with circulating virus (47).

To validate AC_{50} in vaccine evaluation, we compared i.n. infection with PR8 to a single i.m. vaccination, which provides less effective protection against lethal challenge (27). Intramuscular vaccination generates only local GC B cell responses, with inconsistent distal DLN involvement and no splenic resident response (Fig. 6A), pointing to poor trafficking of immunogens (Fig. 6C). Further, GC B cells responding to i.m. versus i.n. vaccination generate B cells with 4-fold less avid AC_{50} at 14 and 28 days postvaccination, despite undergoing a 10-fold affinity increase in the intervening period (Fig. 6D). Together, this suggests while the affinity maturation process remains effective after i.m. vaccination, deficiencies in the early stages of GC formation leads to a smaller and lower-quality starting pool of HA-specific GC B cells. Notably, i.p. immunization with inactivated virus generates a GC B cell response similar to i.n. infection (data not shown), demonstrating that neither infectious virus nor robust viral replication is essential to generate strong responses. A goal of future studies is to better understand the contribution route, dose, and form of immunization to generate optimal B cell responses.

The inferior GC B cell response quantity and quality are supported by serum total binding as determined by SPR analysis

(maximum resonance units [RU]) and dissociation off-rates (Fig. 6F), where serum Ab concentration and quality following vaccination are also lower than after infection. Based on the small HA GC B cell response (5% and 7% of the infected response at 14 and 28 dpi, respectively), we were surprised to note a much smaller disparity in serum Ab concentration (38% and 17% lower at 14 and 28 dpi, respectively). This same disparity in quality is also noted between AC_{50} and serum off-rates, but to a much lower extent (average 4-fold-higher AC_{50} compare to 1.4-fold-lower serum Ab off-rate). These observations clearly highlight the complexities in using cellular response information to predict serum Ab characteristics, where unclear relationships of GC to plasma cells, per-cell antibody production variability, and the contribution of GC-independent Ab responses collectively muddy the waters. Further, the contribution of Ab on-rates to affinity maturation is also unknown.

Further refining of this technique to interrogate the antibody-secreting B cell compartment will enable us to better explore the relationship between the GC B cell response and the serum antibody compartment. To date, we have been unable to specifically stain permeabilized cells with rHA probes, but we have not exhausted all possible combinations of fixing and permeabilizing reagents, particularly given the high rate at which the latter are being introduced. Further, it might be possible to capture secreted antibodies by a chimeric reagent that binds Ig with one arm and an abundant B cell surface molecule with another arm, as has been developed for cytokine analysis (48).

When different vaccine formulations/regimens are being compared, one aim is always to obtain high titers of Abs with high affinity. However, it is not trivial to dissect polyclonal Ab avidities with the technologies available today. SPR analysis is a useful method that can provide off-rates of serum Abs of unknown concentrations. The AC_{50} method presented here should facilitate analysis of Ab avidity in many research laboratories and during initial optimizations of vaccine preparations.

In summary, we describe a simple method to simultaneously quantitate HA-reactive GC B cells while providing a reasonably accurate measure of their Ab affinity. This approach can potentially facilitate the rational design and improvement of vaccines for viruses and other important immunogens.

MATERIALS AND METHODS

rHA^{PR8}. Recombinant PR8 Mount Sinai hemagglutinin (rHA^{PR8}) was expressed and purified as previously described (19, 36). The PR8 HA protein possessed a C-terminal thrombin cleavage site, a "foldon" sequence, and a His tag at the extreme C terminus for protein purification and detection. In later experiments, we also used a PR8 HA with a Y98F mutation that abrogates binding activity with a biotin C-terminal tag (19). For Biacore serum affinity measurements, we used recombinant PR8 H1N1 HA obtained through BEI Resources (NIAID).

Antibody reagents. Allophycocyanin (APC)-conjugated and purified mouse anti-6×His (clone AD 1.1.10) was purchased from Abcam. Fluorescein isothiocyanate (FITC)-conjugated rat anti-mouse CD38 (90/CD38), APC- and phycoerythrin (PE)-conjugated rat anti-mouse GL7 (GL7), PE-Cy7- and Pacific blue-conjugated rat anti-mouse CD45R/B220 (RA3-6B2), and Pacific blue-conjugated hamster anti-mouse CD3ε (500A2) were purchased from BD Biosciences. APC-conjugated streptavidin was purchased from eBioscience. DyLight 6470-conjugated AffiniPure goat anti-mouse IgG (all subclasses), Fcγ fragment specific, was purchased from Jackson ImmunoResearch.

Mice. C57BL/6 mice were purchased from Taconic Farms or Charles River Laboratories. For all experiments, 6- to 12-week-old $AID^{-/-}$ mice (25) were kindly provided by A. Nussenzweig with gracious permission of T. Honjo. All mice were housed under specific-pathogen (including murine norovirus [MNV], mouse parvovirus [MPV], and mouse hepatitis virus [MHV])-free conditions. All animal procedures were approved by and performed in accordance with the NIAID and CBER Animal Care and Use Committee guidelines.

Viruses and infections. For intranasal infections, mice were anesthetized in isoflurane and inoculated intranasally with 50 $TCID_{50}$ (50% tissue culture infective doses) of influenza virus A H1N1 PR8 (Mt. Sinai strain) or influenza virus A J1, a PR8 H3 reassortant (49). For i.p. injections, virus was UV irradiated for 4 min, and 4×10^8 $TCID_{50}$ (pre-UV inactivation titer) was administered by intraperitoneal injection. For intramuscular challenge, UV-inactivated virus was mixed at a ratio of 50:50 with Titermax gold adjuvant (Sigma), and 5×10^6 $TCID_{50}$ (pre UV-inactivation titer) were injected bilaterally into the caudal thigh.

Flow-cytometric analysis. At various times after injection/infection, the mediastinal lymph nodes, inguinal lymph nodes, and/or spleens were harvested from euthanized mice. Tissues were dispersed into single-cell suspensions and treated with red blood cell lysis buffer (Sigma) prior to staining with antibodies. In order to account for the number of specific B cells, a low input cell number (on average 10,000 to 20,000 antigen-specific B cells per tube) combined with excess rHA probe and large washing volumes was used. When stained with recombinant HA (rHA), cells were treated with either filtrate-derived (1:20 dilution) or purified (6 mU/ml in RPMI) neuraminidase from *Vibrio cholerae* for 60 min at 37°C in RPMI (Gibco) to remove surface sialic acid from cells. Cells were stained with primary surface antibodies (30 min, 4°C), with a complete nine-step titration of rHA^{PR8} for each experiment (starting at 66 nM down to 0.0066 nM) (60 min 4°C), and finally with anti-6× antibodies (30 min 4°C), to detect rHA^{PR8} binding. Each experiment included appropriate fluorescent minus one (FMO), unstained, and single-stained controls to ensure proper staining and gates that provided the internal controls for the titration. Stained cells were analyzed on an LSR-II flow cytometer (BD Biosciences). For staining with $rHA^{PR8\text{-}Y98F}$ (19), the same procedure was followed but with neuraminidase treatment omitted and with final staining performed using streptavidin-APC conjugated (30 min, 4°C).

AC_{50} determination. Using a titration of rHA^{PR8} probe with J1 (H3N1)-reactive germinal center B cells, the maximal specific binding of the HA^{PR8} probe was established. rHA^{PR8} probe was titrated over a dose range of 66 nM to 0.66 nM, and data were plotted as the frequency of rHA^{PR8} probe-positive GC B cells. Using a single one-site binding with Hill slope calculation, the 50% maximal binding rHA^{PR8} probe concentration was established to evaluate the antigen concentration that stains 50% of the maximum specific population, or AC_{50}. Where noted, the geometric mean fluorescent intensity (MFI) was used instead of percentage of the population. In these experiments, AC_{50} is defined as the antigen concentration staining at 50% of the maximal MFI.

ELISA. Ninety-six-well plates (Immunlon 4HBX) were used to test MAb reactivity. Plates were coated overnight at 4°C with saturating amounts of purified PR8 HA in phosphate-buffered saline (PBS), then washed three times with PBS containing 0.05% (vol/vol) Tween 20, and blocked with PBS–0.5% fetal bovine serum (FBS) for 2 h at room temperature. MAb was titrated from nondetectable to saturating binding and incubated with virus for 2 h at room temperature. Rat anti-mouse kappa conjugated to horseradish peroxidase (Southern Biotech) was used to detect MAb binding. Plates were developed for 5 min using TMB (tetramethylbenzidine) substrate (KPL biomedical) and halted by the addition of 0.1 N HCl, after which plates were read at 450 nm. Ab avidities were determined using Prism software, and all avidities reported demonstrated excellent fit for one-site binding with Hill slope curve fitting ($R^2 > 0.98$).

SPR analysis of serum antibody. Steady-state equilibrium binding of polyclonal sera was monitored at 25°C using a ProteOn surface plasmon resonance biosensor (Bio-Rad Labs). The recombinant functional PR8 H1N1-HA0 (BEI resources) was coupled to a GLC sensor chip using

amine coupling with 100 resonance units (RU) in the test flow cells. Samples of 60 μl of freshly prepared polyclonal sera at various concentrations were injected at a flow rate of 30 μl/min (120-s contact time). Flow was directed over a mock surface to which no protein was bound, followed by the recombinant functional PR8 H1N1-HA0 coupled surface. Responses from the protein surface were corrected for the response from the mock surface and for responses from a separate, buffer-only injection. MAb 2D7 (anti-CCR5) was used as a negative-control antibody in various binding experiments. Binding kinetics for the sera and the data analysis was analyzed using Bio-Rad ProteON manager software (version 2.1.1). Affinity measurements were calculated using the heterogeneous model.

Statistics. Ab avidities were determined using Prism software, and all avidities reported demonstrated excellent fit for one-site binding with Hill slope curve fitting ($R^2 > 0.98$). Significances were calculated by GraphPad Prism (GraphPad Software, Inc.) using unpaired Student's *t* test.

SUPPLEMENTAL MATERIAL

Supplemental material for this article may be found at http://mbio.asm.org/lookup/suppl/doi:10.1128/mBio.01156-15/-/DCSupplemental.

Figure S1, TIF file, 0.4 MB.
Figure S2, TIF file, 0.3 MB.
Figure S3, TIF file, 0.1 MB.

ACKNOWLEDGMENTS

We thank the Comparative Medicine Branch and staff of the NIH as well as the FDA CDER vivariums for their work in maintaining the animal colonies used in these studies.

This work was generously supported by the National Institute of Allergy and Infectious Diseases Division of Intramural Research and Food and Drug Administration Centers for Drug Evaluation and Research.

REFERENCES

1. **Stoop JW, Zegers BJ, Sander PC, Ballieux RE.** 1969. Serum immunoglobulin levels in healthy children and adults. Clin Exp Immunol **4:**101–112.
2. **Eisen HN, Siskind GW.** 1964. Variations in affinities of antibodies during the immune response. Biochemistry **3:**996–1008. http://dx.doi.org/10.1021/bi00895a027.
3. **Victora GD, Nussenzweig MC.** 2012. Germinal centers. Annu Rev Immunol **30:**429–457. http://dx.doi.org/10.1146/annurev-immunol-020711-075032.
4. **McHeyzer-Williams LJ, McHeyzer-Williams MG.** 2005. Antigen-specific memory B cell development. Annu Rev Immunol **23:**487–513. http://dx.doi.org/10.1146/annurev.immunol.23.021704.115732.
5. **Blink EJ, Light A, Kallies A, Nutt SL, Hodgkin PD, Tarlinton DM.** 2005. Early appearance of germinal center-derived memory B cells and plasma cells in blood after primary immunization. J Exp Med **201:**545–554. http://dx.doi.org/10.1084/jem.20042060.
6. **Chan TD, Wood K, Hermes JR, Butt D, Jolly CJ, Basten A, Brink R.** 2012. Elimination of germinal-center-derived self-reactive B cells is governed by the location and concentration of self-antigen. Immunity **37:**893–904. http://dx.doi.org/10.1016/j.immuni.2012.07.017.
7. **Pape KA, Taylor JJ, Maul RW, Gearhart PJ, Jenkins MK.** 2011. Different B cell populations mediate early and late memory during an endogenous immune response. Science **331:**1203–1207. http://dx.doi.org/10.1126/science.1201730.
8. **Wrammert J, Koutsonanos D, Li GM, Edupuganti S, Sui J, Morrissey M, McCausland M, Skountzou I, Hornig M, Lipkin WI, Mehta A, Razavi B, Del Rio C, Zheng NY, Lee JH, Huang M, Ali Z, Kaur K, Andrews S, Amara RR, Wang Y, Das SR, O'Donnell CD, Yewdell JW, Subbarao K, Marasco WA, Mulligan MJ, Compans R, Ahmed R, Wilson PC.** 2011. Broadly cross-reactive antibodies dominate the human B cell response against 2009 pandemic H1N1 influenza virus infection. J Exp Med **208:**181–193. http://dx.doi.org/10.1084/jem.20101352.
9. **Purtha WE, Tedder TF, Johnson S, Bhattacharya D, Diamond MS.** 2011. Memory B cells, but not long-lived plasma cells, possess antigen specificities for viral escape mutants. J Exp Med **208:**2599–2606. http://dx.doi.org/10.1084/jem.20110740.
10. **Wrammert J, Smith K, Miller J, Langley WA, Kokko K, Larsen C, Zheng NY, Mays I, Garman L, Helms C, James J, Air GM, Capra JD, Ahmed R, Wilson PC.** 2008. Rapid cloning of high-affinity human monoclonal antibodies against influenza virus. Nature **453:**667–671. http://dx.doi.org/10.1038/nature06890.
11. **Gerhard W, Mozdzanowska K, Furchner M, Washko G, Maiese K.** 1997. Role of the B-cell response in recovery of mice from primary influenza virus infection. Immunol Rev **159:**95–103. http://dx.doi.org/10.1111/j.1600-065X.1997.tb01009.x.
12. **Puck JM, Glezen WP, Frank AL, Six HR.** 1980. Protection of infants from infection with influenza A virus by transplacentally acquired antibody. J Infect Dis **142:**844–849. http://dx.doi.org/10.1093/infdis/142.6.844.
13. **Molinari NA, Ortega-Sanchez IR, Messonnier ML, Thompson WW, Wortley PM, Weintraub E, Bridges CB.** 2007. The annual impact of seasonal influenza in the US: measuring disease burden and costs. Vaccine **25:**5086–5096. http://dx.doi.org/10.1016/j.vaccine.2007.03.046.
14. **Beigel JH.** 2008. Influenza. Crit Care Med **36:**2660–2666. http://dx.doi.org/10.1097/CCM.0b013e318180b039.
15. **Gerhard W.** 2001. The role of the antibody response in influenza virus infection. Curr Top Microbiol Immunol **260:**171–190. http://dx.doi.org/10.1007/978-3-662-05783-4_9.
16. **Doucett VP, Gerhard W, Owler K, Curry D, Brown L, Baumgarth N.** 2005. Enumeration and characterization of virus-specific B cells by multicolor flow cytometry. J Immunol Methods **303:**40–52. http://dx.doi.org/10.1016/j.jim.2005.05.014.
17. **Onodera T, Takahashi Y, Yokoi Y, Ato M, Kodama Y, Hachimura S, Kurosaki T, Kobayashi K.** 2012. Memory B cells in the lung participate in protective humoral immune responses to pulmonary influenza virus reinfection. Proc Natl Acad Sci U S A **109:**2485–2490. http://dx.doi.org/10.1073/pnas.1115369109.
18. **Bardelli M, Alleri L, Angiolini F, Buricchi F, Tavarini S, Sammicheli C, Nuti S, Degl'Innocenti E, Isnardi I, Fragapane E, Del Giudice G, Castellino F, Galli G.** 2013. *Ex vivo* analysis of human memory B lymphocytes specific for a and B influenza hemagglutinin by polychromatic flow-cytometry. PLoS One **8:**e70620. http://dx.doi.org/10.1371/journal.pone.0070620.
19. **Whittle JR, Wheatley AK, Wu L, Lingwood D, Kanekiyo M, Ma SS, Narpala SR, Yassine HM, Frank GM, Yewdell JW, Ledgerwood JE, Wei CJ, McDermott AB, Graham BS, Koup RA, Nabel GJ.** 2014. Flow cytometry reveals that H5N1 vaccination elicits cross-reactive stem-directed antibodies from multiple Ig heavy-chain lineages. J Virol **88:**4047–4057. http://dx.doi.org/10.1128/JVI.03422-13.
20. **Magadán JG, Khurana S, Das SR, Frank GM, Stevens J, Golding H, Bennink JR, Yewdell JW.** 2013. Influenza A virus hemagglutinin trimerization completes monomer folding and antigenicity. J Virol **87:**9742–9753. http://dx.doi.org/10.1128/JVI.00471-13.
21. **Price PW, McKinney EC, Wang Y, Sasser LE, Kandasamy MK, Matsuuchi L, Milcarek C, Deal RB, Culver DG, Meagher RB.** 2009. Engineered cell surface expression of membrane immunoglobulin as a means to identify monoclonal antibody-secreting hybridomas. J Immunol Methods **343:**28–41. http://dx.doi.org/10.1016/j.jim.2009.01.005.
22. **Oracki SA, Walker JA, Hibbs ML, Corcoran LM, Tarlinton DM.** 2010. Plasma cell development and survival. Immunol Rev **237:**140–159. http://dx.doi.org/10.1111/j.1600-065X.2010.00940.x.
23. **Shimizu T, Oda M, Azuma T.** 2003. Estimation of the relative affinity of B cell receptor by flow cytometry. J Immunol Methods **276:**33–44. http://dx.doi.org/10.1016/S0022-1759(03)00068-1.
24. **Kavaler J, Caton AJ, Staudt LM, Schwartz D, Gerhard W.** 1990. A set of closely related antibodies dominates the primary antibody response to the antigenic site CB of the A/PR/8/34 influenza virus hemagglutinin. J Immunol **145:**2312–2321.
25. **Muramatsu M, Kinoshita K, Fagarasan S, Yamada S, Shinkai Y, Honjo T.** 2000. Class switch recombination and hypermutation require activation-induced cytidine deaminase (AID), a potential RNA editing enzyme. Cell **102:**553–563. http://dx.doi.org/10.1016/S0092-8674(00)00078-7.
26. **Zaheen A, Boulianne B, Parsa JY, Ramachandran S, Gommerman JL, Martin A.** 2009. AID constrains germinal center size by rendering B cells susceptible to apoptosis. Blood **114:**547–554. http://dx.doi.org/10.1182/blood-2009-03-211763.
27. **Harris K, Ream R, Gao J, Eichelberger MC.** 2011. Intramuscular immunization of mice with live influenza virus is more immunogenic and offers greater protection than immunization with inactivated virus. Virol J **8:**251. http://dx.doi.org/10.1186/1743-422X-8-251.

28. **Virelizier JL**. 1975. Host defenses against influenza virus: the role of anti-hemagglutinin antibody. J Immunol **115:**434–439.
29. **Whittle JR, Zhang R, Khurana S, King LR, Manischewitz J, Golding H, Dormitzer PR, Haynes BF, Walter EB, Moody MA, Kepler TB, Liao HX, Harrison SC**. 2011. Broadly neutralizing human antibody that recognizes the receptor-binding pocket of influenza virus hemagglutinin. Proc Natl Acad Sci U S A **108:**14216–14221. http://dx.doi.org/10.1073/pnas.1111497108.
30. **Roost HP, Bachmann MF, Haag A, Kalinke U, Pliska V, Hengartner H, Zinkernagel RM**. 1995. Early high-affinity neutralizing anti-viral IgG responses without further overall improvements of affinity. Proc Natl Acad Sci U S A **92:**1257–1261. http://dx.doi.org/10.1073/pnas.92.5.1257.
31. **Fazekas de St. Groth S**. 1967. Cross recognition and cross reactivity. Cold Spring Harb Symp Quant Biol **32:**525–536.
32. **Jerne NK**. 1985. The generative grammar of the immune system. Science **229:**1057–1059. http://dx.doi.org/10.1126/science.4035345.
33. **Yewdell JW**. 2003. He put the id in idiotype. EMBO Rep **4:**931–1004. http://dx.doi.org/10.1038/sj.embor.embor951.
34. **Ennis FA, Yi-Hua Q, Schild GC**. 1982. Antibody and cytotoxic T lymphocyte responses of humans to live and inactivated influenza vaccines. J Gen Virol **58:**273–281. http://dx.doi.org/10.1099/0022-1317-58-2-273.
35. **Yewdell JW**. 1981. The study of influenza virus antigens by means of monoclonal hybridoma antibodies. University of Pennsylvania, Philadelphia, PA.
36. **Yang H, Chen LM, Carney PJ, Donis RO, Stevens J**. 2010. Structures of receptor complexes of a North American H7N2 influenza hemagglutinin with a loop deletion in the receptor binding site. PLoS Pathog **6:**e1001081. http://dx.doi.org/10.1371/journal.ppat.1001081.
37. **Elsner RA, Ernst DN, Baumgarth N**. 2012. Single and coexpression of CXCR4 and CXCR5 identifies CD4 T helper cells in distinct lymph node niches during influenza virus infection. J Virol **86:**7146–7157. http://dx.doi.org/10.1128/JVI.06904-11.
38. **Boyden AW, Legge KL, Waldschmidt TJ**. 2012. Pulmonary infection with influenza A virus induces site-specific germinal center and T follicular helper cell responses. PLoS One **7:**e40733. http://dx.doi.org/10.1371/journal.pone.0040733.
39. **Bessa J, Zabel F, Link A, Jegerlehner A, Hinton HJ, Schmitz N, Bauer M, Kündig TM, Saudan P, Bachmann MF**. 2012. Low-affinity B cells transport viral particles from the lung to the spleen to initiate antibody responses. Proc Natl Acad Sci U S A **109:**20566–20571. http://dx.doi.org/10.1073/pnas.1206970109.
40. **Zinkernagel RM**. 2002. On differences between immunity and immunological memory. Curr Opin Immunol **14:**523–536. http://dx.doi.org/10.1016/S0952-7915(02)00367-9.
41. **Fazekas de Saint Groth S, Webster RG, Davenport FM**. 1969. The antigenic subunits of influenza viruses. I. The homologous antibody response. J Immunol **103:**1099–1106.
42. **Khurana S, Verma N, Yewdell JW, Hilbert AK, Castellino F, Lattanzi M, Del Giudice G, Rappuoli R, Golding H**. 2011. MF59 adjuvant enhances diversity and affinity of antibody-mediated immune response to pandemic influenza vaccines. Sci Transl Med **3:**85ra48. http://dx.doi.org/10.1126/scitranslmed.3002336.
43. **Hedman K, Hietala J, Tiilikainen A, Hartikainen-Sorri AL, Räihä K, Suni J, Väänänen P, Pietiläinen M**. 1989. Maturation of immunoglobulin G avidity after rubella vaccination studied by an enzyme linked immunosorbent assay (avidity-ELISA) and by haemolysis typing. J Med Virol **27:**293–298. http://dx.doi.org/10.1002/jmv.1890270407.
44. **Wilson PC, Andrews SF**. 2012. Tools to therapeutically harness the human antibody response. Nat Rev Immunol **12:**709–719. http://dx.doi.org/10.1038/nri3285.
45. **Burton DR, Poignard P, Stanfield RL, Wilson IA**. 2012. Broadly neutralizing antibodies present new prospects to counter highly antigenically diverse viruses. Science **337:**183–186. http://dx.doi.org/10.1126/science.1225416.
46. **Finn JA, Crowe JE, Jr.** 2013. Impact of new sequencing technologies on studies of the human B cell repertoire. Curr Opin Immunol **25:**613–618. http://dx.doi.org/10.1016/j.coi.2013.09.010.
47. **Osterholm MT, Kelley NS, Sommer A, Belongia EA**. 2012. Efficacy and effectiveness of influenza vaccines: a systematic review and meta-analysis. Lancet Infect Dis **12:**36–44. http://dx.doi.org/10.1016/S1473-3099(11)70295-X.
48. **List T, Neri D**. 2013. Immunocytokines: a review of molecules in clinical development for cancer therapy. Clin Pharmacol Adv Appl **5:**29–45. http://dx.doi.org/10.2147/CPAA.S49231.
49. **Caton AJ, Koprowski H**. 1990. Influenza virus hemagglutinin-specific antibodies isolated from a combinatorial expression library are closely related to the immune response of the donor. Proc Natl Acad Sci U S A **87:**6450–6454. http://dx.doi.org/10.1073/pnas.87.16.6450.